Science of the Total Environment 652 (2019) 177–188

Contents lists available at ScienceDirect

Science of the Total Environment

journal homepage: www.elsevier.com/locate/scitotenv

Spatial and vertical distribution of ^{129}I and ^{127}I in the East China Sea: Inventory, source and transportation

Jinlong Wang [a], Yukun Fan [b], Dantong Liu [a], Tong Lu [b], Xiaolin Hou [b,c], Jinzhou Du [a,*]

[a] State Key Laboratory of Estuarine and Coastal Research, East China Normal University, Shanghai 200062, PR China
[b] State Key Laboratory of Loess and Quaternary Geology, Xi'an AMS Center, Institute of Earth Environment, CAS, 710061 Xi'an, PR China
[c] Center for Nuclear Technologies, Technical University of Denmark, Risø Campus, Roskilde 4000, Denmark

HIGHLIGHTS

- Iodine-129 is useful for understanding water mass movement in the ocean.
- $^{129}I/^{127}I$ atomic ratios varied with the water mass in the East China Sea.
- Oceanic input dominates the ^{129}I inventory.
- Vertical profiles of ^{129}I provide information for studying mixing processes.
- $^{129}I/^{127}I$ is useful for tracing the water mass exchange and land-sea interaction.

GRAPHICAL ABSTRACT

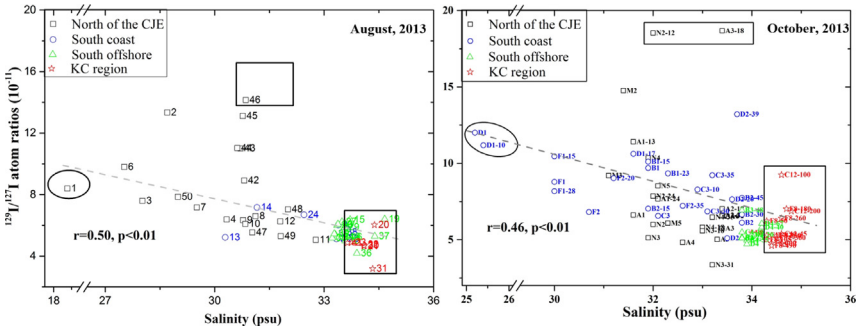

ARTICLE INFO

Article history:
Received 23 July 2018
Received in revised form 17 October 2018
Accepted 17 October 2018
Available online 18 October 2018

Editor: Mae Sexauer Gustin

Keywords:
$^{129}I/^{127}I$
Vertical profile
Water mass
Mixing process
Marginal sea

ABSTRACT

Iodirne-129 is useful for tracking water mass movement in the ocean. In this study, the concentration of iodine isotopes in seawater of the East China Sea (ECS) in October 2013 were analyzed to investigate the spatial and vertical distribution of ^{129}I and ^{127}I to understand water mass exchange. Results showed that the $^{129}I/^{127}I$ atomic ratios varied with the water mass, with higher values of (10–20) $\times 10^{-11}$ in the coastal regions and lower values of $<8 \times 10^{-11}$ offshore. Inventories of ^{129}I were estimated to be (0.23–1.7) $\times 10^{12}$ atoms m^{-2} ($n = 18$) in upper 100 m waters, which is comparable to those of other regions without being contaminated by the nuclear accidents or nuclear reprocessing facilities. The total amount of ^{129}I in the ECS water column was estimated to be 88 g in which over 90% is attributed to the oceanic input (e.g., West Pacific) via the Kuroshio Current (KC). The contributions of ^{129}I from Changjiang (Yangtze River) terrestrial watershed (<7.5%) and atmospheric fallout (<2.7%) were small. Those from the Fukushima accident were negligible during this investigation. The $^{129}I/^{127}I$ ratios versus salinity distribution showed the range and stratification of the Changjiang, Yellow Sea, and KC waters in the ECS. Our study shows that the Changjiang fresh water could be transported to the North Jiangsu coast in October; the Taiwan Warm Current water could intrude to Northern part of the Changjiang Estuary (32°N). Besides, our results suggest that the $^{129}I/^{127}I$ profile is useful to indicate the seawater mixing process in ocean marginal systems.

1. Introduction

Iodine-129 (^{129}I) (with a half-life of 15.7 myr) in the environment is derived from both natural processes (250 kg) (cosmic ray reactions

* Corresponding author.
E-mail address: jzdu@sklec.ecnu.edu.cn (J. Du).

https://doi.org/10.1016/j.scitotenv.2018.10.248
0048-9697/

with xenon and the fission of uranium), and anthropogenic processes, such as thermonuclear bomb testing (50–150 kg), nuclear accidents (e.g., Chernobyl (1.3–6 kg) and Fukushima (1.2 kg)), nuclear power plants and nuclear reprocessing facilities (6500 kg, mainly contributed by La Hague, France and Sellafield, UK) (Aldahan et al., 2007a; Hou et al., 2009, 2013; He et al., 2013a, b). Considering its long half-life and relatively low beta-energy (with a maximum beta-emitted energy of 154 keV), ^{129}I is not very radiologically harmful. Instead, ^{129}I is widely utilized as a tracer for the biogeochemical cycle of iodine, the movement and exchange of water masses, and the interactions between atmosphere and seawater in marine environments (Hou et al., 2007; Zhang and Hou, 2013; Xing et al., 2017). Due to its high solubility (K_d: 5–30 L kg^{-1}, Takata et al., 2013) and long residence time in the ocean (~300 kyr) compared to the turnover time of ocean water (~1 kyr, Broecker and Peng, 1982), ^{129}I can be utilized to trace the cycling of insoluble organic carbon and phytoplankton blooms associated with reductive conditions (Schwehr et al., 2005; Hou and Hou, 2012; Liu D. et al., 2016).

Iodine-127 (^{127}I) is a stable isotope, and ^{129}I/^{127}I atomic ratios (described as ratios in this study) largely vary depending on the source of iodine in the marine environment. These ratios range from 3×10^{-12} to 2×10^{-6}, which are higher than the prenuclear level (1.5×10^{-12}) (Fehn et al., 2000; Xing et al., 2017). Therefore, ^{129}I/^{127}I ratio is very useful for identifying the source of ^{129}I and for tracing water mass movements in marine environments. For example, in the Irish Sea and the North Sea, the extremely high ^{129}I/^{127}I ratios in seawater (~10^{-6}) were attributed to discharge from two nuclear fuel reprocessing plants at La Hague (France) and Sellafield (UK) (Raisbeck et al., 1995; Hou et al., 2007; Michel et al., 2012). Meanwhile, iodine isotopes have also been used to trace the movement of sea currents from the coast of Northern Europe to the Arctic Ocean (Hou et al., 2000; Alfimov et al., 2004a). In the coastal ocean and marginal sea, water masses usually vary seasonally, especially in coastal areas strongly affected by monsoons (e.g., the seasonally variable coastal currents) and they show different features in vertical profiles, e.g., the Kuroshio Current has different temperature and salinity characteristics in its surface and subsurface (Ichikawa and Beardsley, 2002). Thus, defining the spatiotemporal and vertical distributions of iodine isotopes in seawater is of fundamental importance for their effective use as tracers.

The East China Sea (ECS), as a typical ocean marginal sea, contains oceanic input currents, seasonally variable coastal currents, and large river inputs. Previous studies show that the turnover time of the ECS shelf water was approximately 1.3 yr and that times of coastal and estuarine waters were much lower at approximately 30 days (Tan et al., 2018; Wang et al., 2018); these times are significantly lower than the residence time of ^{129}I in ocean water. ^{129}I is still highly soluble in estuaries (K_d: <200 L kg^{-1}, Takata et al., 2013), and thus, can be used to trace the exchange of water masses in marginal seas, even with abundant sediment discharge from rivers. Vertical profiles associated with the estimated inventory and spatial distribution of ^{129}I and ^{127}I are relevant to the long-range transport of other conservative-behavior radionuclides (e.g., ^{3}H, ^{90}Sr, ^{137}Cs and U isotopes) and oceanic currents. In recent years, increased numbers of nuclear power plants (NPPs) have been constructed along the coast of the ECS, such as Qinshan in Haiyan City, Tianwan in Lianyungang City, and Sanmen in Taizhou City. The potential releases of anthropogenic radionuclides, including iodine isotopes, from these NPPs to the environment have aroused profound concern. Thus, it is necessary to determine the baseline of concentrations of ^{129}I and ^{127}I, and movement in the ECS, which can provide vital information for evaluating the possible impacts of these NPPs.

Some studies have reported the concentrations of ^{129}I and ^{127}I in the seawater of marginal systems in the Northwestern Pacific (e.g., Cooper et al., 2001; Povinec et al., 2013; Casacuberta et al., 2017); however, the time-series and vertical profiles of two isotopes are still limited, especially in the ECS (Suzuki et al., 2010; Hou et al., 2013). In our previous work (Liu D. et al., 2016), by observing the spatial distribution of iodine isotopes (i.e., ^{129}I and ^{127}I) concentration and species in the seawater of the ECS in August, we found that ^{129}I decreased from the coast to offshore. Additionally, the species of ^{129}I and ^{127}I were dominated by iodate in the shelf water, but existed mainly as iodide in the Changjiang (Yangtze River) Estuary. We also found that the influence of the Fukushima nuclear accident on the ^{129}I level of the ECS was not detectable until August 2013. In this work, we extended our research to focus on the inventory and temporal changes of ^{129}I and ^{127}I; we also quantified the source of ^{129}I in the ECS seawater by observing the spatial distribution and vertical profile of ^{129}I. The temporal distribution pattern can be established by combining with the data from our previous study (Liu D. et al., 2016). The aim of this study is to test the use of iodine isotopes in tracing water mass exchanges and mixing processes in the marginal sea. These results are expected to promote our understanding of not only the movement of iodine isotopes in estuarine and continental shelf areas, but also the long-term transport of other conservative radionuclides by oceanic current.

2. Materials and methods

2.1. Study area

The ECS has one of the broadest continental shelves in the world, is a river-dominated marginal sea located between the Asian continent and the Pacific Ocean (Fig. 1). The north border of the ECS is defined by the line connecting Qidong and Cheju Island. The southern boundary is from west to the east and aligned with the southern part of Taiwan Strait, and the east border is the Ryukyu Islands and Taiwan Island. The ECS is ~400 km long and has a maximum width of ~640 km, with a mean and maximum water depth of 349 m and 2719 m, respectively. The ECS shelf is relatively flat, slanting from the continental shelf toward the southeast, with a mean gradient of 0.04% (Wang et al., 2016). There are >40 rivers flowing into the ECS, including the largest river in China and the third-largest river in the world (Changjiang) that discharges abundant sediment and freshwater to the ECS. Due to the heavy influence of monsoons, there are two seasonally variable coastal currents that are impacted by the Changjiang Diluted Water (CDW). The Yellow Sea Coastal Current (YSCC) and the Zhejiang–Fujian Coastal Current (ZFCC) are southward-flowing in winter and spring, but they reverse or even disappear in summer. The CDW flows southward in winter and spring, but northeastward in summer. In the northern region of the ECS, the YSCC intersects with the northward Yellow Sea Warm Current (YSWC) and forms a loop current. From the open sea side, there are two northward-flowing currents, i.e., the Taiwan Warm Current (TWC) and the Kuroshio Current (KC). The KC is one branch of the boundary current in the Western Pacific, which comprises surface, subsurface, intermediate and deep-water regions. The surface water of the KC ranges from 80 m to 200 m and the subsurface water is below the surface water, with a maximum depth of 450 m; it is characterized by a high salinity (~35 psu) (Ichikawa and Beardsley, 2002).

2.2. Sampling and analysis

Seawater samples, including 26 surface seawater samples (<2 m in depth) and 18 vertical profiles, were collected during the R/V "Dongfanghong 2" cruise between October 11th and November 6th, 2013. Among these samples, there were three (i.e., M2, M3 and M5) collected in the Southern Yellow Sea. After collection, the samples were filtered (Φ 0.45 μm) in situ and stored in 2 L polyethylene plastic bottles in the dark for subsequent laboratory analyses. Temperature and salinity of the seawater samples were measured in situ during sampling. Iodine isotopes data collected from the surface seawater samples during August 2013 were reported in our previous study (Liu D. et al., 2016) (Fig. 2).

The method for iodine separation from seawater was modified from Hou et al. (2010). Briefly, 1000 mL of filtered seawater was placed in a beaker and spiked with 0.2 mg of ^{127}I carrier (Woodward iodine,

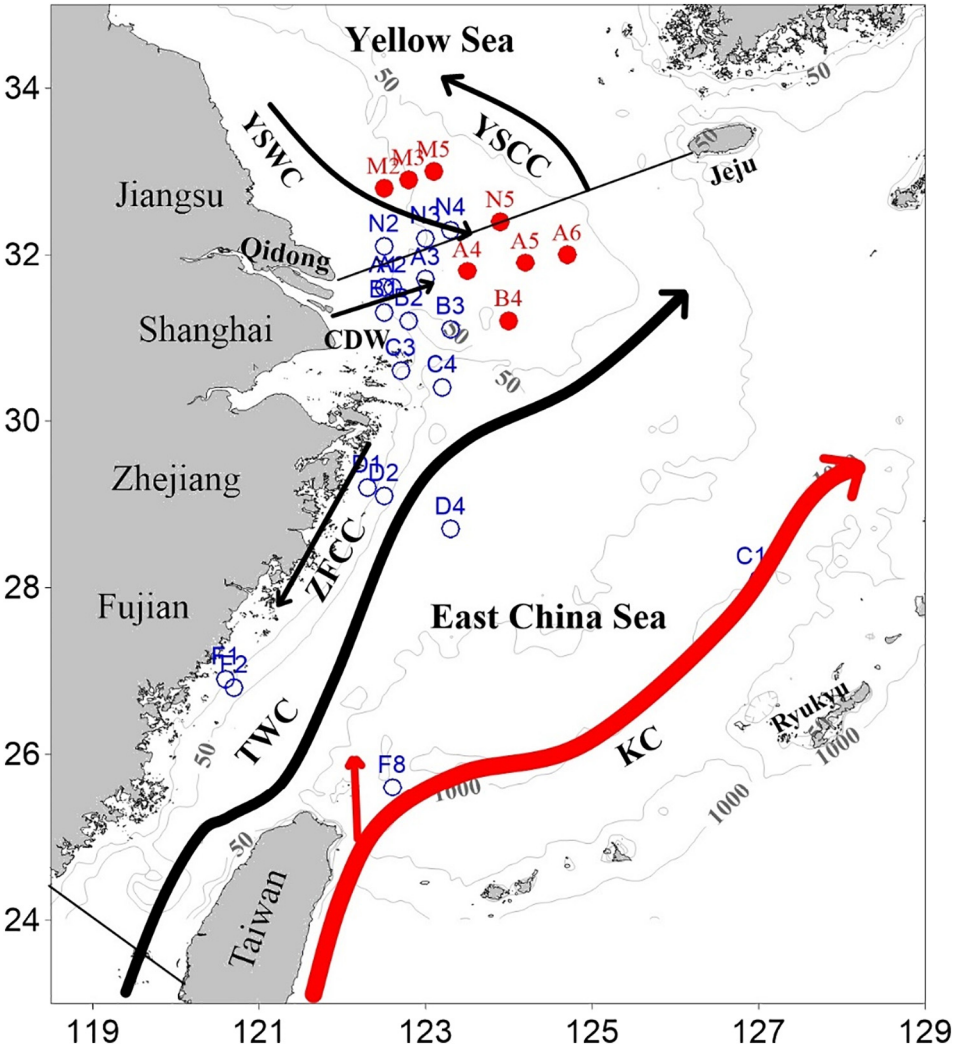

Fig. 1. Location of sampling stations in the ECS during the October cruise in 2013 (surface water in red and vertical profiles in blue). The regional surface current in the autumn is modified after Wu H. et al., 2014; Wu J. et al., 2014: Yellow Sea Coastal Current (YSCC); Yellow Sea Warm Current (YSWC); Changjiang Dilute Water (CDW); Zhejiang-Fujian Coast Current (ZFCC); Taiwan Warm Current (TWC); Kuroshio Current (KC). The bathymetry (m) of the ECS shelf is shown by grey lines. The boundary of the ECS is shown by black lines.

Woodward Iodine Corporation, Oklahoma, USA) and 200 Bq ^{125}I; then, 0.50 mL of 2.0 mol L^{-1} $NaHSO_3$ solution was added. Then, 6 mol L^{-1} HNO_3 was added to adjust the pH to <2 to convert the iodine species to iodide. A total of 28 mL of 0.01 mol L^{-1} $AgNO_3$ solution was slowly added while stirring to coprecipitate iodide as AgI-AgCl. After the supernatant was discarded, the AgI-AgCl precipitate was separated by centrifuge and sequentially rinsed with 3 mol L^{-1} HNO_3, H_2O, and 7.5%, 2.5%, and 1% $NH_3 \cdot H_2O$ to remove Ag_2SO_3 and excessive AgCl and AgBr until 1–3 mg of precipitate was obtained for AMS measurements. The chemical yield of iodine in the chemical separation was obtained by measuring the ^{125}I in the precipitate using a NaI gamma detector (Model FJ-2021, Xi'an Nuclear Instrument factory, Xi'an, China) and was found to be 85–95%. Procedural blanks were prepared using the same procedures as the samples. These blanks contained deionized water instead of samples. Only inorganic iodine was separated from the seawater, and the reported results of ^{129}I are only for inorganic species. Since the organic iodine only accounts for a very small fraction of iodine in open sea water (Hou et al., 1999), the reported inorganic ^{129}I might also represent total ^{129}I in the seawater, except for a very few samples from the estuary region.

The separated AgI–AgCl coprecipitate was dried in an oven at 60–70 °C, homogeneously pulverized, and mixed with niobium powder (325-mesh, Alfa Aesar, Ward Hill, MA) in a 1:5 mass ratio. The mixture was pressed into a copper holder using a pneumatic press (Zhenjiang Aode Presser Instruments Ltd.). The $^{129}I/^{127}I$ atomic ratios in the prepared targets were measured by AMS using a 3MV Tandem AMS system (HVEE) in the Xi'an AMS center. All $^{127}I^{5+}$ ions were measured as charges (current) using a Faraday cup, and $^{129}I^{5+}$ was measured using a gas ionization detector. All samples were measured for 6 cycles, with 5 min per sample in each cycle. The procedural background $^{129}I/^{127}I$ ratio was measured to be 1.0×10^{-13}, which is approximately two orders of magnitude lower than that measured in the samples. The measurement uncertainty for the samples was <3.5% (Liu D. et al., 2016). A detailed description of the AMS system and ^{129}I measurements was reported by Hou et al. (2010).

The concentration of ^{127}I in seawater was measured by ICP-MS (Thermo Scientific, X series II, USA) after undergoing a 10-time dilution using a 1% ammonium solution. Samples were spiked with Cs^+ (2 ng mL^{-1}), which was also used as an internal standard. The detection limit of ^{127}I was determined to be 0.02 ng mL^{-1}, which is >2 orders of magnitude lower than its measured value in the diluted seawater.

3. Results

3.1. The spatial distribution of iodine isotopes in the ECS

Iodine isotopes, temperature and salinity values in the surface water of the ECS are listed in the Supplemental file (Table S1). The ^{127}I

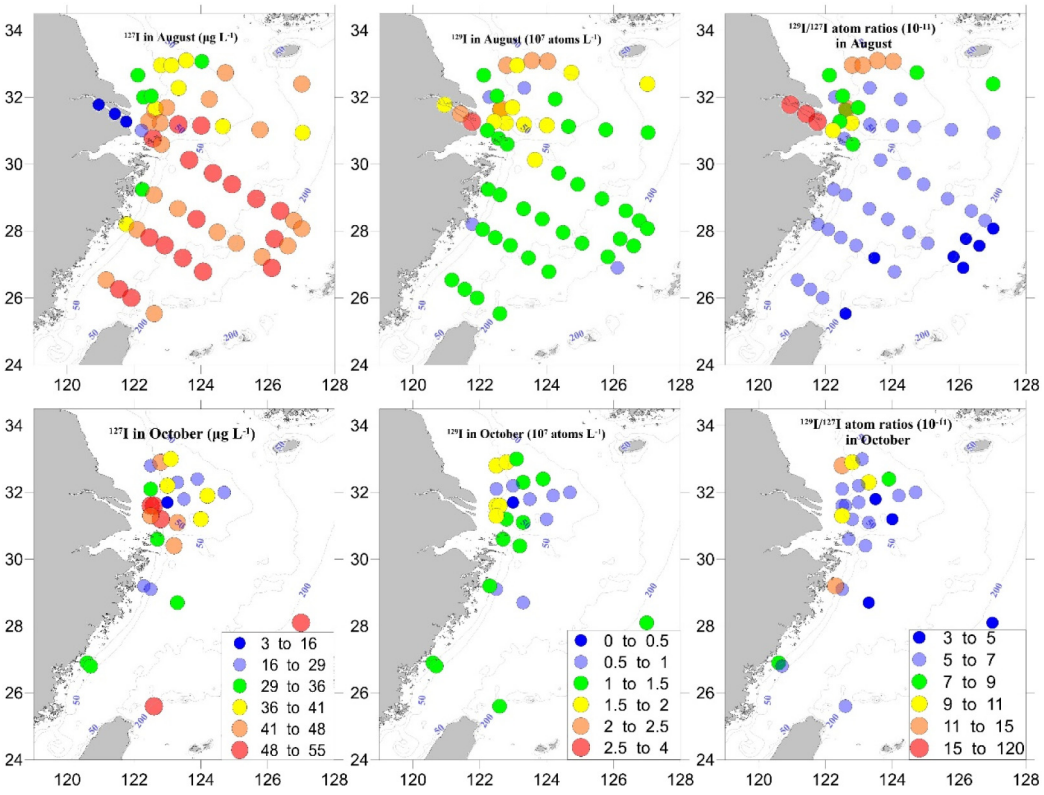

Fig. 2. Spatial distribution of ^{127}I and ^{129}I concentrations and $^{129}I/^{127}I$ atoms ratios in the surface water in the ECS during August (replotted from Liu D. et al., 2016) and October of 2013.

concentrations in surface seawater ranged from 15.6 to 54.7 μg L^{-1} (mean of 33.2 ± 1.7 μg L^{-1}, n = 26) in October, which were similar to those observed in August (Fig. 2). The lowest ^{127}I concentrations were observed near the Changjiang Estuary, ranging from 15.6 to 25.0 μg L^{-1}- and are comparable to the values in the water in August of the same year (Fig. 2). The lower ^{127}I concentrations in the Changjiang Estuary are attributed to the freshwater input with low ^{127}I from the Changjiang River. Even lower ^{127}I concentrations of 3.1–7.1 μg L^{-1} were observed in the three locations of the inner part of the Changjiang Estuary. The maximum values of ^{127}I were found in the southeastern region of the ECS, and this trend was the same as that in August. However, the concentrations of ^{127}I in the northeastern region of the ECS were much lower in October (26.0–38.5 μg L^{-1}) than those in August (41.8–47.4 μg L^{-1}). The October ^{129}I concentrations in the surface seawater of the ECS are (0.61–1.94) × 10^7 atoms L^{-1} (mean of (1.22 ± 0.09) × 10^7 atoms L^{-1}, n = 26) and were slightly lower than those in August. However, this value was 1–2 orders of magnitude higher than the prenuclear level of 0.043 × 10^7 atoms L^{-1} (Snyder et al., 2010). The spatial distribution pattern of ^{129}I was the opposite of that of ^{127}I, i.e., ^{129}I was higher in the Changjiang Estuary, but relatively lower in the offshore seawater. The measured ^{129}I concentrations in the surface seawater in this study were comparable to the reported values in surface water of the North Pacific (20°N–45°N) ((0.59–3.7) × 10^7 atoms L^{-1}) (Guilderson et al., 2014), Japan Sea ((0.28–5.8) × 10^7 atoms L^{-1}) (Cooper et al., 2001), and southern Indian Ocean ((0.60–0.80) × 10^7 atoms L^{-1}) (Povinec et al., 2011), however, they were higher than concentrations in the Antarctic region ((0.11–0.31) × 10^7 atoms L^{-1}) (Xing et al., 2017), lower than in the Bering Sea ((1.8–131) × 10^7 atoms L^{-1}) (Cooper et al., 2001) and North Atlantic (31°N–50°N) ((4.0–127) × 10^7 atoms L^{-1}) (He et al., 2013a, b), and much lower than in the Baltic Sea ((0.25–17) × 10^{10} atoms L^{-1}) (Yi et al., 2010), North Sea ((0.26–38) × 10^{10} atoms L^{-1}) (Hou et al., 2007), Celtic Sea ((0.03–1.2) × 10^{10} atoms L^{-1}) (He et al., 2014) and Irish Sea ((6.2–47) × 10^{10} atoms L^{-1}) (Schnabel et al., 2007), where they were heavily contaminated by the discharge from the reprocessing plants at La Hague (France) and Sellafield (UK).

The $^{129}I/^{127}I$ ratios in the surface seawater collected in October 2013 varied from 4.72 × 10^{-11} to 14.7 × 10^{-11} (mean of (7.02 ± 0.49) × 10^{-11}, n = 26) and were significantly lower than those observed in August but were more than one order of magnitude higher than the prenuclear level (1.5 × 10^{-12}, Snyder et al., 2010). The distribution pattern of $^{129}I/^{127}I$ is similar to the ^{129}I concentrations, which means that the ^{129}I concentrations dominate the distribution pattern of $^{129}I/^{127}I$ ratios. The maximum values of $^{129}I/^{127}I$ ratios were found in the estuary area in both seasons (Fig. 3). The second-highest $^{129}I/^{127}I$ ratios (~1.6 × 10^{-11}) were found in the Jiangsu Coast in both seasons. In the northeastern region of the ECS, the $^{129}I/^{127}I$ ratios were higher in August (>1.2 × 10^{-11}) than those in October (<0.9 × 10^{-11}). $^{129}I/^{127}I$ ratios in the freshwater of the Changjiang were much higher (~100 × 10^{-11}) than those in the coastal areas of the ECS (Liu D. et al., 2016). This can be attributed to the $^{129}I/^{127}I$ ratio of the Changjiang input being largely diluted by high ^{127}I concentration seawater when the land-sourced ^{129}I (with low ^{127}I level) water is transported southward along the coast (Wu et al., 2013; Wang et al., 2016). Additionally, when freshwater of the Mississippi River was discharged into the coastal area of continental Louisiana, the $^{129}I/^{127}I$ ratios were decreased from 113 × 10^{-11}–519 × 10^{-11} (Oktay et al., 2001) to 16 × 10^{-11}–41 × 10^{-11} (Schwehr et al., 2005).

3.2. The vertical profiles of iodine isotopes in the water column

The vertica.l profile of iodine isotopes in the sampling stations in the ECS are plotted in Fig. 3. In section N (Fig. 3), narrow variations of ^{127}I concentrations were observed at all three stations. ^{129}I concentrations showed a maximum value (2.5 × 10^7 atoms L^{-1}) at a depth of 12 m at station N2; the maximum value of the $^{129}I/^{127}I$ ratio was also found in the same layer of N2. Similar trends were also found at stations A1 and A3, where the ^{127}I and ^{129}I concentrations decreased from surface

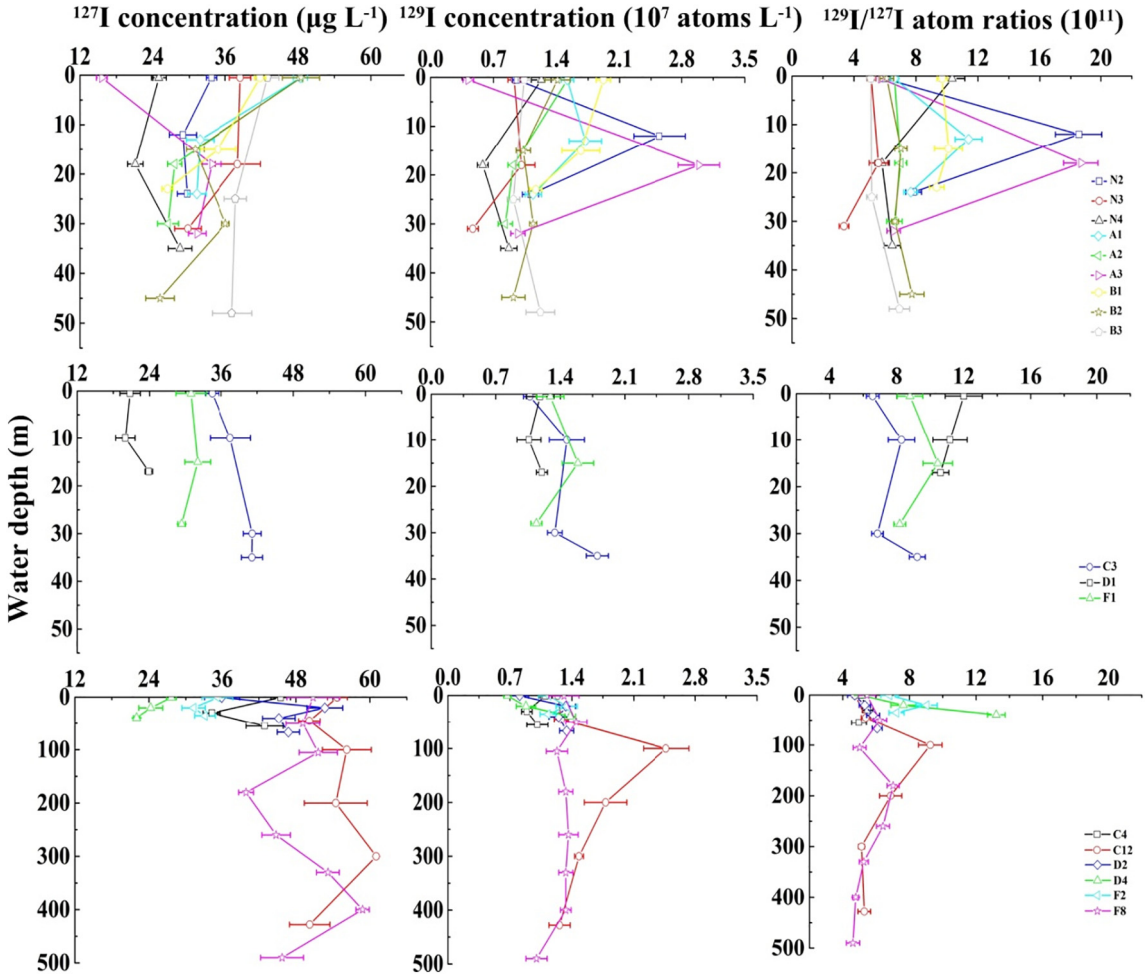

Fig. 3. The vertical profiles of ^{127}I and ^{129}I concentrations and ^{129}I/^{127}I atom ratios in the ECS water column during October of 2013. The iodine isotopes distributions are plotted as three group for different regions: Northern part of the Changjiang river mouth, inner shelf the ECS and offshore region.

to bottom water, but the ^{129}I/^{127}I ratios were relatively constant. In section B, the ^{127}I concentrations first increased and then decreased with increasing depth at the two stations (i.e., B1 and B2) near the river mouth, but they were constant at station B3. The ^{129}I concentrations showed a narrow variation with depth at stations B2 and B3, but they decreased from the surface water to the bottom layer at station B1. The ^{129}I/^{127}I ratios decreased from the surface waters to the 25-m layers at three stations, and the maximum values decreased from B1 to B2.

In sections C, D, and F (Fig. 3), there are six stations located in coastal areas and two stations (F8 and C12) located in the pathway of the KC. In the coastal areas, the concentrations of ^{129}I and ^{127}I varied little at different depths that indicates the vertical profiles of iodine isotopes associated with the water mass were well-mixed in the water column in these areas. The uniform vertical distributions of temperature and salinity (Table S1) also support this statement. In addition, the ^{129}I/^{127}I ratios in the depth profile were constant at stations C4 and D1, but they showed higher values at the bottom layers at stations C3 (9.2×10^{-11}) and D2 (13×10^{-11}). Relatively higher values were also observed in the 17-m layers of stations F1 and F2. In an offshore station (i.e., D4) through which the TWC flows, the ^{129}I/^{127}I ratios were constant, and temperature and salinity also showed a very narrow range of variation. In the margin of the ECS shelf where the KC flows, the ^{127}I concentrations of seawater showed higher values (40–60 μg L^{-1}) in the vertical profiles at stations F8 and C12. The highest values were found in the 300-m and 400-m layers at stations F8 and C12, respectively. The ^{129}I concentrations at station F8 showed relatively minor variation, but those at station C12 showed a maximum value in the 100-m layer and then decreased with increasing depth. The ^{129}I/^{127}I atomic ratios were constant at the surface layer and then reached their highest values at the 100-m layer at station C12 and the 180-m layer at station F8.

4. Discussions

4.1. The inventory of ^{129}I in the ECS water column

The inventory of ^{129}I (I, atoms m^{-2}) in the seawater column can be estimated using the following equation (modified from Suzuki et al., 2010):

$$I_x = \sum_{i=1}^{n-1} \frac{1}{2}\left({}^{129}C_{i+1} + {}^{129}C_i\right)(d_{i+1} - d_i) + {}^{129}C_1 d_1 + {}^{129}C_n(d_b - d_n) \quad (1)$$

where n is the sampling depth. $^{129}C_i$ represents the concentrations (atoms m^{-3}) of ^{129}I in seawater at depth i. d_i and d_b refer to the ith sampling depth of seawater (m) and the total depth to the bottom (m, total depth of the water column), respectively. The inventories of ^{129}I were estimated to be (0.23–0.79) $\times 10^{12}$ atoms m^{-2} (mean of (0.46 ± 0.15) $\times 10^{12}$ atoms m^{-2}) in shallow waters (27–65 m in total depth) and (6.5–7.3) $\times 10^{12}$ atoms m^{-2} (mean of (6.9 ± 0.6) $\times 10^{12}$ atoms m^{-2}) in deep waters (440–500 m in total depth) (Table 1 and Fig. 4). The inventories of ^{129}I in the shallow waters generally increased from the coasts to the offshore region. The deeper stations hold a higher

inventory because they have more volume of water compared to shallow stations or shelf stations. To understand the sources and sinks of ^{129}I, here we only compared the inventory in first 100 m depth of the water column with other regions in the world. Generally, the inventories of ^{129}I in the upper 100 m water column of the ECS were comparable to those of the North Pacific ((1.7–3) × 10^{12} atoms m^{-2}) (Povinec et al., 2010; Suzuki et al., 2010), the Southern Indian Ocean ((0.6–0.8) × 10^{12} atoms m^{-2}) (Povinec et al., 2011) and the Gulf of Mexico (1.5 × 10^{12} atoms m^{-2}) (Schink et al., 1995), which suggest a similar dominant source initially from the global fallout for these regions. However, the results from the ECS were clearly lower than those from the offshore of Fukushima ((8–24) × 10^{12} atoms m^{-2}) (Hou et al., 2013), and the enhanced values observed in the offshore of Fukushima are attributed to the release from the Fukushima accident. The Arctic Ocean ((3.4–141) × 10^{12} atoms m^{-2}) (Smith et al., 1998; Alfimov et al., 2004a) and Baltic Sea ((60–6834) × 10^{12} atoms m^{-2}) (Alfimov et al., 2004b; Aldahan et al., 2007a) also had very high ^{129}I inventories compared to the ECS. The ^{129}I concentration in the upper 100 m water column of the North Atlantic Ocean (6 × 10^{7} atoms L^{-1} to 4.7 × 10^{11} atoms L^{-1}) (Edmonds et al., 2001; Schnabel et al., 2007; Alfimov et al., 2004c, 2013) was also much higher than that of the ECS, and thus the ^{129}I inventories are expected be much higher than those of the ECS. The enhanced ^{129}I inventories in the Arctic

Table 1
Comparison of the ^{129}I inventory in water columns. The data in bracket represents the ^{129}I inventory calculated for the upper 100 m water column.

Sample	Longitude	Latitude	Sampling date	Water depth (m)	^{129}I (×10^{12} atoms m^{-2})	References
East China Sea						
N4	32.3N	123.3E	2013/10/13	38	0.31 ± 0.03	This study
N3	32.2N	123.0E	2013/10/14	37	0.30 ± 0.04	
N2	32.1N	122.5E	2013/10/14	27	0.46 ± 0.04	
A1	31.6N	122.5E	2013/10/17	27	0.40 ± 0.03	
A2	31.6N	122.6E	2013/10/17	34	0.36 ± 0.03	
A3	31.7N	123.0E	2013/10/17	35	0.61 ± 0.05	
B3	31.1N	123.3E	2013/10/20	51	0.53 ± 0.04	
B2	31.2N	122.8E	2013/10/20	49	0.54 ± 0.04	
B1	31.3N	122.5E	2013/10/20	26	0.23 ± 0.06	
C3	30.6N	122.7E	2013/10/27	38	0.54 ± 0.04	
C4	30.4N	123.2E	2013/10/27	59	0.58 ± 0.06	
D4	28.7N	123.3E	2013/10/30	65	0.79 ± 0.07	
D2	29.1N	122.5E	2013/10/31	46	0.47 ± 0.04	
D1	29.2N	122.3E	2013/10/31	22	0.25 ± 0.02	
F1	26.9N	120.6E	2013/11/3	32	0.44 ± 0.04	
F2	26.8N	120.7E	2013/11/5	39	0.48 ± 0.04	
C12	28.1N	127.0E	2013/10/29	440	7.3 ± 0.4 (1.7 ± 0.2)	
F8	25.6N	122.6E	2013/11/6	501	6.5 ± 0.3 (1.4 ± 0.1)	
Japan Basin	41.0N	138.0E	2007/8/11	3623	23 (<2)	Suzuki et al., 2010
Yamato Basin	38.5N	135.0E	2007/8/11	2966	18 (<3)	
Offshore of Kushiro	42.1N	146.2E	2007/8/11	5694	7 (<1.7)	
Offshore of Fukushima						
11	37.5N	147.0E	2011/6/9	400	24 ± 0.2 (11 ± 0.1)	Hou et al., 2013
14	37.5N	144.0E	2011/6/10	400	15 ± 0.2 (8.4 ± 0.1)	
22	38.0N	143.0E	2011/6/13	400	43 ± 1.8 (15 ± 1)	
31	37.5N	141.4E	2011/6/15	120	24 ± 0.4	
Northwest Pacific						
Sts. 2	34.92N	151.91E	1997/10/26	6100	27 ± 3 (<2.1)	
Sts. 3	30.57N	170.61E	1997/10/30	5470	36 ± 4 (<2.3)	Povinec et al., 2010
Southern Indian Ocean						
Sts. 3	45.66S	63.11E	1999/01	4320	21 ± 4 (0.6 ± 0.1)	Povinec et al., 2011
Sts. 7	44.01S	64.73E	1999/01	4551	22 ± 4 (0.7 ± 0.1)	
Sts. 8	42.91S	63.08E	1999/01	4998	30 ± 6 (0.8 ± 0.1)	
Western Arctic Ocean						
B			1993	3000	185 ± 30 (4.5 ± 05)	Smith et al., 1998
TA			1993	300	88 ± 3 (4.3 ± 0.4)	
TC			1993	600	206 ± 7 (22 ± 1)	
D			1993	2150	403 ± 32 (3.4 ± 0.5)	
E			1993	2000	634 ± 29 (82 ± 2)	
Eastern Arctic Ocean						
Nansen Basin	83.28N	31.95E	2001.07	1000	511 ± 30 (117 ± 7)	Alfimov et al., 2004a
Amundsen Basin	88.41N	95.38E	2001.07	3900	927 ± 53 (127 ± 6)	
Makarov Basin	87.92N	154.38E	2001.07	3500	493 ± 27 (141 ± 6)	
Baltic Sea						
A	58.41N	11.2E	2000–2001	23	1361 ± 62	Aldahan et al., 2007b
B	58.53N	11.22E	2000–2001	23	1288 ± 86	
C	58.61N	11.25E	2000–2001	15	841 ± 42	
D	58.65N	11.03E	2000–2001	134	6834 ± 325	
E	58.80N	11.08E	2000–2001	242	6952 ± 439 (3914 ± 235)	
F	59.05N	11.15E	2000–2001	97	4237 ± 235	
G	59.08N	11.37E	2000–2001	35	1392 ± 73	
H	59.02N	11.42E	2000–2001	12	382 ± 23	
1	58.0N	20.1E	1999/02	125	373 ± 15	Alfimov et al., 2004b
2	59.0N	21.1E	1999/02	150	356 ± 10	
3	61.1N	19.6E	1999/02	100	60 ± 2	
Gulf of Mexico	26.7N	95.0W	1992/3/18	1510	4.7 (1.5 ± 0.2)	Schink et al., 1995

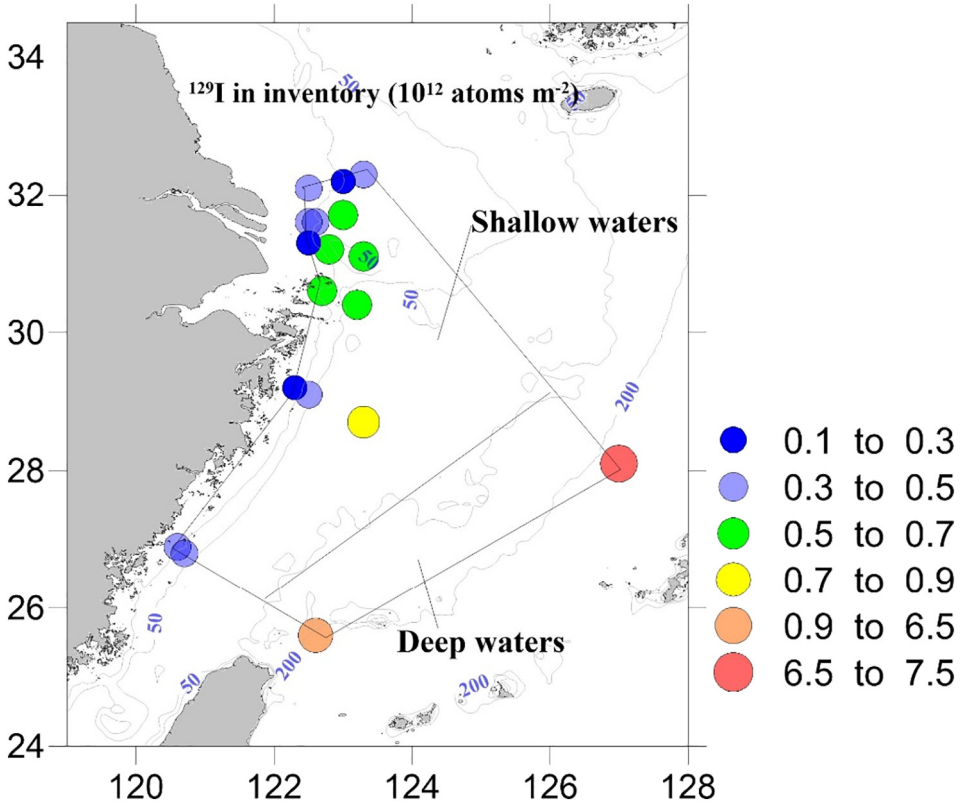

Fig. 4. Spatial distribution of ^{129}I inventories in water column in the ECS during October of 2013. The shallow and deep waters are dived by the 100-m isobaths.

and the North Atlantic Ocean were attributed to the marine discharge of ^{129}I from the nuclear reprocessing facilities at La Hague and Sellafield (Alfimov et al., 2004c). Overall, the inventory estimation could offer a good approach to check whether if there are extra sources than global fallout, or other sources.

4.2. Sources and sinks of ^{129}I in the ECS

In the use of ^{129}I as tracers for the assessment of water mass in marginal sea, its source terms should be first assessed. ^{129}I in the ECS is initially from the atmospheric fallout released from the weapon tests before 1970 and reprocessing plants Sellafield (UK) and La Hague (France) during 1970s and 1990s (Fan et al., 2016; Bautista et al., 2016; Zhang et al., 2018). Radionuclides from the source entered the ECS by means of river input, direct atmospheric deposition, and/or ocean currents (Liu D. et al., 2016). Our previous study suggested that the main sources of ^{129}I in the water column of the ECS are riverine input, atmospheric fallout, and oceanic input (including adjacent sea and open sea inputs), but their contributions were not quantified (Liu D. et al., 2016). The sinks of ^{129}I are mainly storage within the water column and sedimentary deposition.

The total amount of ^{129}I in the water column of the ECS was estimated based on the inventory of ^{129}I. Due to the dramatic differences in the ^{129}I inventory between shallow and deep waters, it is more reasonable to separately calculate the total ^{129}I in these waters. The total surface area of the ECS corresponding to the ^{129}I inventories was estimated using Google Earth to be 2.56×10^{11} m^2 that was divided into two parts by the 100-m isobaths (2.185×10^{11} m^2 for the shallow waters and 4.65×10^{10} m^2 for the deep waters) (Fig. 6). Based on this the total ^{129}I in the water column of the ECS can be estimated to be $(4.2 \pm 0.4) \times 10^{23}$ atoms (88 g) using the mean inventory in the two layers ($(0.46 \pm 0.15) \times 10^{12}$ atoms m^{-2} for the shallow waters (<100 m) and $(6.9 \pm 0.6) \times 10^{12}$ atoms m^{-2} for the deep waters (400–500 m)) with each corresponding surface area. This value is far smaller than those in the water column of the nuclear reprocessing facilities (La Hague, France and Sellafield, UK) contaminated seas, including the Baltic Sea (15 kg), North Sea (86 kg), Nordic Sea (1100 kg), Barnets Sea (366 kg) and Kara Sea (113 kg) (Aldahan et al., 2007a). As the turnover time of the ECS shelf water was ~1.3 yrs. (Wang et al., 2018), the total flux of ^{129}I stored in the water column was estimated to be $(3.2 \pm 0.3) \times 10^{23}$ atoms y^{-1} using the total ^{129}I ($(4.2 \pm 0.4) \times 10^{23}$ atoms) divided by the turnover time of the ECS.

4.2.1. Sources of ^{129}I in the ECS

The concentrations of the dissolved ^{129}I in the inner region of the Changjiang Estuary were reported to be $(1.7–4.0) \times 10^7$ atoms L^{-1} (mean of $(2.6 \pm 1.2) \times 10^7$ atoms L^{-1}, n = 3) during August 2013 (Liu D. et al., 2016). Using this mean value and the annual water discharge of the Changjiang to the ECS (9.05×10^{11} m^3 yr^{-1}) (Yang et al., 2015), the mean annual ^{129}I input derived from the Changjiang water is $(2.4 \pm 1.1) \times 10^{22}$ atoms, which is much lower than the inventory of ^{129}I in the ECS. Since there are no reported data about the particulate ^{129}I in the Changjiang water, here, we used a simple equation to roughly estimate the ^{129}I input (I_{sed}, atmos yr^{-1}) via sediment discharge from the Changjiang as follows:

$$I_{sed} = I_{wat} \times TSM \times K_d \quad (2)$$

where I_{wat} is the ^{129}I input by water discharge from the Changjiang ($(2.4 \pm 1.1) \times 10^{22}$ atoms yr^{-1}). TSM is the mean concentration of total suspended matter discharged from the Changjiang to the ECS (1.4×10^{-4} ton m^{-3}) that was estimated by dividing the annual sediment discharge (1.3×10^8 ton yr^{-1}) (Yang et al., 2015) by the water discharge of the Changjiang. The K_d of iodine was reported to be 40–200 m^3 ton^{-1} in the estuaries (Takata et al., 2013). Considering that the mean TSM of the Changjiang is very high, here, the

maximum value (200 m^3 ton^{-1}) was used. Finally, the I_{sed} is estimated to be (6.8 ± 3.2) × 10^{20} atoms yr^{-1}, which is very small (~3% of I_{wat}) compared to the total inventory of ^{129}I (<0.2% of the total inventory of ^{129}I in the ECS). Overall, the contribution of ^{129}I from the Changjiang riverine input to the ECS is just a small fraction (7.5%) of the total flux of ^{129}I in the water column ((3.2 ± 0.3) × 10^{23} atoms yr^{-1}) of the ECS, although the CDW significantly affects the seasonal variation of ^{129}I in the water column near the Changjiang Estuary. Since the total discharge from other rivers only contributes 10% of freshwater to the ECS (Milliman and Farnsworth, 2013), the input of ^{129}I from these rivers to the ECS is <0.75% of the total inventory assuming that the ^{129}I concentrations in these rivers are the same as those in the Changjiang.

Direct atmospheric fallout should also contribute ^{129}I to the ECS. Although there are no reported data for deposition to the ECS, other data from the nearest stations at the same latitude as the ECS, i.e., Tokyo to the north (35.5°N) and Ishigaki Island to the south (24.0°N) were used. During the Fukushima accident, the westerly wind brought and deposited most of the released ^{129}I in the northern North Pacific Ocean (Tumey et al., 2014; Casacuberta et al., 2017), causing negligible deposition in the ECS. The ^{137}Cs in the seawater collected in the ECS after the Fukushima accident confirmed this (Zhao et al., 2018). These investigations revealed that the ^{129}I released from the Fukushima accident was mainly deposited on land and in the offshore waters near the Fukushima NPP, resulting in a very small influence on the sea areas of southwest Japan (Hou et al., 2013; Casacuberta et al., 2017). Thus, the preaccident ^{129}I deposition data from Tokyo and Ishigaki Island can be used to roughly estimate the contribution of direct atmospheric fallout to the ECS. Toyama et al. (2013) estimated that the atmospheric depositional ^{129}I in Tokyo was 6.2 × 10^{10} atoms m^{-2} yr^{-1} during 2003 and that in Ishigaki Island was 0.69 × 10^{10} atoms m^{-2} yr^{-1} at 2003. By multiplying the median of ^{129}I deposition (3.4 × 10^{10} atoms m^{-2} yr^{-1}) for the two stations with the surface area of the ECS (2.56 × 10^{11} m^2), the atmospheric fallout of ^{129}I to the ECS was 0.087 × 10^{23} atoms yr^{-1}. This value accounts for approximately 3% of the total ^{129}I flux in the water column of the ECS.

4.2.2. ^{129}I budget in the ECS

Due to the high solubility and long residence time of iodine in the ocean, reports of concentrations in marine sediments are very limited, especially in the marginal seas of the NW Pacific (Fan et al., 2016). This makes the estimation of the sedimentary deposition of ^{129}I difficult for the ECS. However, considering the low TSM in the ECS (<10 mg L^{-1}) and the lower K_d values (<30 L kg^{-1}) of ^{129}I in seawater relative to those in estuaries (Huang et al., 2013; Takata et al., 2013), the amount of ^{129}I buried in ECS sediment should be small compared to that stored in the water column. The ^{129}I inventories in water column were reported to be ten times higher than those buried in the sediments from the North Sea, Nordic Sea, and North Atlantic Ocean (Aldahan et al., 2007a). Without considering the sedimentary buried ^{129}I in the ECS, a lower limit ((2.9 ± 0.3) × 10^{23} atoms yr^{-1}) of net input of ^{129}I was obtained from the Northwest Pacific via the KC and TWC and the Yellow Sea via the YWCC (Fig. 5) that represents approximately 90% of the flux of ^{129}I in the ECS. A previous study suggested that the oceanic input of Pu from the Pacific Proving Ground (PPG) in the Northwest Pacific dominated the mass balance of Pu in the ECS sediment and that a small portion of Pu was likely derived from the Yellow Sea (Wang et al., 2017). It is reasonable that the very conservative ^{129}I could be transported from the Northwest Pacific to the ECS and that some portion of ^{129}I could be derived from the Yellow Sea via the YSCC.

4.3. Implication of $^{129}I/^{127}I$ for tracing water mass movement

4.3.1. The potential use of $^{129}I/^{127}I$ as a tracer for identifying the water mass in the ECS

Multicurrents and biological activities (e.g., enrichment by phytoplankton) could affect the distribution of iodine isotopes in the ECS (Butler et al., 1981; Liu D. et al., 2016). The ^{129}I concentrations decreased from the coast to offshore, whereas ^{127}I is mainly oceanic, and its concentration distribution showed a reverse pattern relative to ^{129}I and generally increased with salinity ($r = 0.53$, $p < 0.01$). The $^{129}I/^{127}I$ ratios could help alleviate biological effects on the iodine isotopes' concentration distribution, and thus are more significant than single iodine isotopes in tracing the exchange of water masses in the ECS. The $^{129}I/^{127}I$ ratios showed very weak linear correlation with the salinity ($r = -0.46$, $p < 0.01$). This implies that the ECS waters do not result from the simple two-endmember (fresh and salt water) mixing (Fig. 6a). Instead, three main endmembers can be identified in October 2013: the CDW water, YSCC water and KC water, which are characterized by the salinity and $^{129}I/^{127}I$ ratios of <25 and 12 × 10^{-11}, 32.5 and 18 × 10^{-11}, 35.5 and 6 × 10^{-11}, respectively. The highest $^{129}I/^{127}I$ ratios were observed in the middle layer of the water column at stations A3 and N3. These values are similar to those of surface sediments ((177–189) × 10^{-12}) at Jiaozhou Bay in the Yellow Sea (Fan et al., 2016). Relatively high concentrations of ^{129}I were also observed in the surface water of the northernmost region of the ECS (stations M2 and M3). Therefore, the high ^{129}I contents in the middle layer at stations A3 and N3 may have originated from the Yellow Sea water, which flows southward and downwards to the middle layer of the northern ECS (Lie et al., 2000). The $^{129}I/^{127}I$ ratios versus salinity distribution in the KC waters showed a distinct pattern (with the highest salinities and relatively lower $^{129}I/^{127}I$ ratios) compared to other regions. It is noted that the water derived by the KC and TWC cannot be separated by $^{129}I/^{127}I$ ratios and salinity, and thus they are considered as one source.

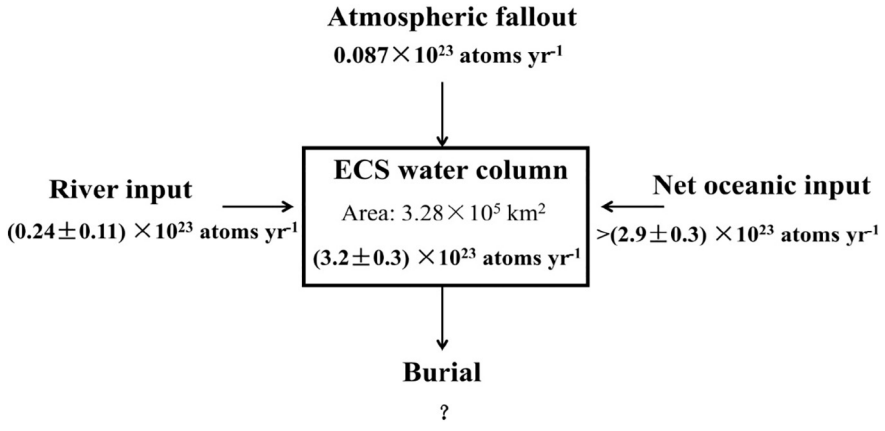

Fig. 5. The mass balance of ^{129}I in the seawater of the ECS.

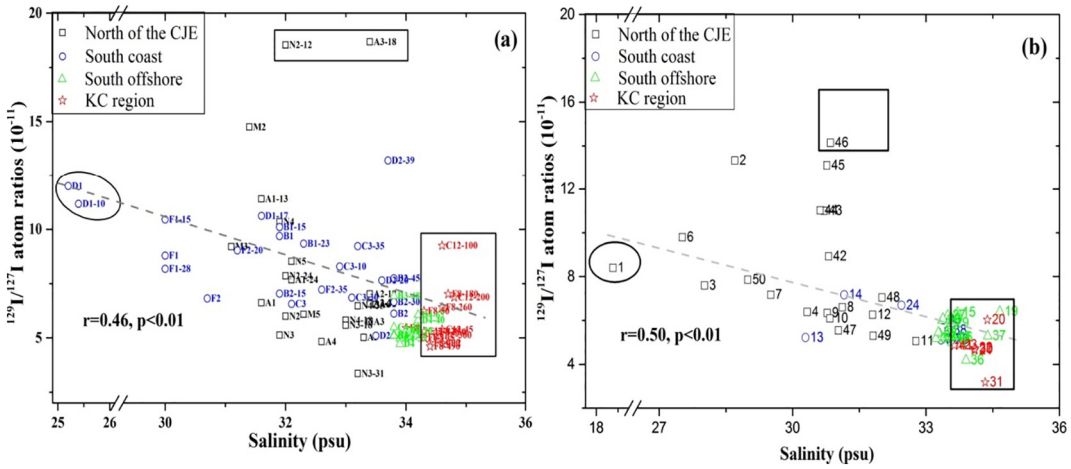

Fig. 6. Distribution of $^{129}I/^{127}I$ atom ratios vs. salinity in seawater of the ECS during October (a) and August (b) 2013. CJE represents the Changjiang Estuary.

From Fig. 6a, the upper 10 m of water at station D1 seems to be derived from the CDW waters, and surface water at station F1 showed the similar salinity and $^{129}I/^{127}I$ ratios. This suggests that CDW-derived water could transport southward to F1 via the ZFCC during October. While at the bottom layer of the station D1, the salinity and $^{129}I/^{127}I$ ratio lay in the middle range of CDW water and KC water values. This suggests mixing between these two endmembers. At station D2, the 39-m layer water showed a mixing signal between YSCC water and KC water that is similar to a recent in situ observation conducted nearby (28°N, 122°E) during February and March 2014. Liu et al. (2018) deduced the YS water could be transported to the ECS. Our result suggests that the YSCC water might also be transported to the inner shelf (29°N, 122°E) of the ECS during October via the intermediate or near-bottom layer water. In the south offshore (east of 30 m isobath), the spatial and vertical distribution of $^{129}I/^{127}I$ ratios were dominated by the KC input, which brings abundant warm and salty water associated with lower $^{129}I/^{127}I$ ratios iodine isotopes to the coastal areas (Guo et al., 2006; Zhang et al., 2017). The $^{129}I/^{127}I$ ratios versus the salinity distribution of surface water during August 2013 showed a similar pattern to those during October, indicating that three sources are impacting ratios. However, the $^{129}I/^{127}I$ ratios versus salinity both in the south coast and offshore of the ECS showed the signal close to the KC water, reflecting a stronger intrusion of the TWC and KC to coastal areas of the ECS during summer relative to autumn. From Fig. 6a, the KC waters could intrude into the inner shelf near the Zhe-Min Coast and Changjiang Estuary via the bottom layer (Ichikawa and Beardsley, 2002).

The source of the water mass in the north of the ECS is very complex due to the joint interaction of the multicurrent, tide, monsoon, and topography. Wu H. et al. (2014) hypothesized that a small portion of the CDW plume could extend along the Jiangsu coast in winter that is mainly driven by the tide-induced Stokes drift. The CDW waters signal were also observed in the surface water of the Jiangsu coast both in October (e.g., stations M2), suggesting that such an extension of the CDW plume might also exist in autumn. The signal of Changjiang input was also found in other parameters of sediment in the Jiangsu coast, e.g., its magnetic minerals, trace elements and clay minerals (Zhang et al., 2012; Lu et al., 2015). These observations further suggest that Changjiang-derived iodine isotopes can be transported to the Jiangsu coast via the tide-induced coastal current (e.g., autumn and winter). From Fig. 6, the iodine isotopes in the north of the ECS are derived from the mixing of the CDW, YSCC, and KC waters. Lian et al. (2016) used $\delta^{18}O$ and δD as tracers to suggest that the subsurface waters of the KC could intrude near the Changjiang river mouth. In this study, the $^{129}I/^{127}I$ ratios versus salinity distribution showed that the KC (and TWC) water could arrive at the north part (32°N, 123°E) of the Changjiang Estuary (e.g., station 48, 49 and N2). As mentioned above, the signal of YSCC water was observed in the intermediate layer of the northern ECS (i.e., N2 and A3). However, for the surface water, the $^{129}I/^{127}I$ ratios versus salinity distribution showed a mixing between CDW water and the KC/TWC water. This indicates that an upwelling originating from the KC/TWC water meeting the shallower topography in the Changjiang Estuary (31°N, 122.5°E) mixed with the CDW plume and being transported northward. Furthermore, the signal of the KC water was also observed in bottom layer of the station N3 and N4, which further suggests the complex structure of multicurrent in the northern ECS.

Overall, the spatial and vertical distribution of iodine isotopes is significantly affected by the complex current system in the ECS. The $^{129}I/^{127}I$ ratios-traced water mass structure in the ECS is shown in Fig. 7. Assessing the land-sea interactions of nutrients, especially the estimation of oceanic contributions via the KC, has consistently been one of the most difficult and important scientific problems in river-influenced marginal systems (Liu S.M. et al., 2016). Our study showed that the $^{129}I/^{127}I$ ratio is sensitive to water mass exchange in the ECS and that most ^{129}I is originated from oceanic input; thus, the $^{129}I/^{127}I$ ratio could serve as a good indicator for better tracing the land-sea interactions of nutrients in marginal systems.

4.3.2. Implication of $^{129}I/^{127}I$ for seawater vertical mixing process

The vertical profiles of both $^{129}I/^{127}I$ ratios and ^{129}I concentrations generally showed narrow variations in south offshore waters with depths between 30 m and 100 m (Fig. 3), indicating the vertical mixing of seawater in the middle shelf of the ECS or a similar source of well mixed water. In a station offshore Fukushima (31), significantly higher ^{129}I concentrations were observed in the top 20-m waters during June 2011 (Hou et al., 2013); this depth likely represents a mixing layer during a 3-month timescale after the Fukushima accident. In deep waters of the offshore ECS (e.g., F8 and C12), the $^{129}I/^{127}I$ ratios and ^{129}I concentrations showed fluctuations in the vertical profiles. The maximum ratio was observed in the subsurface water (100-m depth) at station C12, located at the major pathway of the KC (e.g., C12). The maximum values of the $^{129}I/^{127}I$ ratio in the water column were also found in the 25-m-deep water of the Middle Atlantic Bight (36–37°N) in 1993 (Santschi et al., 1996), and the existence of maximum ^{90}Sr and ^{137}Cs concentrations in subsurface water was also observed in the central NW Pacific Ocean (Povinec et al., 2003; Hong et al., 2012). Buesseler and Livingston (1997) used the subsurface Cs maximum which corresponded to Chernobyl fallout to indicate the vertical mixing process near the Bosporus, Black Sea. Biological activity might affect the species components (iodate and iodide) of ^{129}I, but it exerts less influence on the vertical distribution of $^{129}I/^{127}I$ ratios (Zhang and Hou, 2013). Instead, physical circulation and the specific sourced water

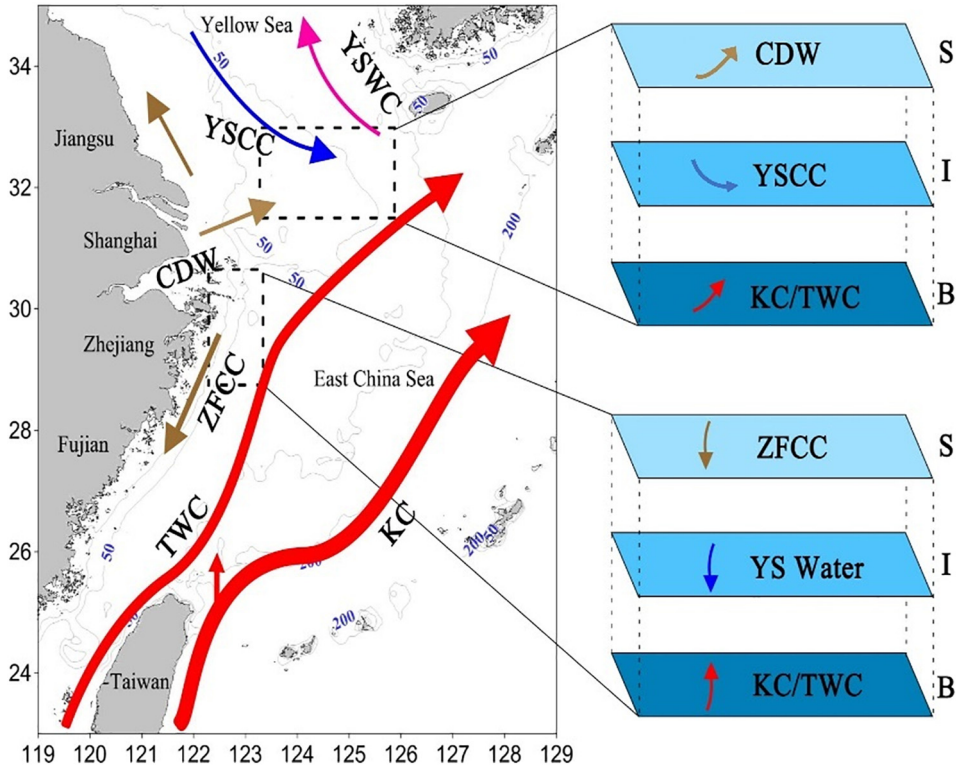

Fig. 7. Diagram of the water mass structure in the ECS during October traced by the $^{129}I/^{127}I$ ratios. S, I and B represent the surface waters, intermediate waters and bottom waters in the ECS, respectively.

might play an important role in the existence of the subsurface maximum $^{129}I/^{127}I$ ratios. It is well known that the nuclear weapons tests in the PPG released a large amount of radioactive substance to the marine system. A component of radionuclides was deposited and buried in the sediment of the local area; the resuspension and/or re-emission of these radionuclides from the sediment to the water body has become the major source of these radionuclides in the upper water. A remarkable signal of plutonium in the seawater and sediment in the East and South China Seas has been observed, which is attributed to the KC that carried a PPG sourced signal to this region (Wu J. et al., 2014; Wang et al., 2017). The subsurface maximum of the ^{129}I signal in the offshore water column at station C12 might be attributed to the source from the PPG. Since iodine is highly soluble in seawater compared to the particle-reactive plutonium, this signal is a good indicator of the PPG source water mass in this region.

5. Conclusions

Based on the results of surface waters at 26 stations and water column at 18 stations in the ECS, the inventory, source and transportation of iodine isotopes were investigated. The inventories of ^{129}I were estimated to be $(0.23–0.79) \times 10^{12}$ atoms m^{-2} ($n = 16$) in shallow waters (<100 m) and $(6.5–7.3) \times 10^{12}$ atoms m^{-2} ($n = 2$) in deep waters (400–500 m). The ^{129}I inventories of upper 100 m waters in the ECS were comparable to (significantly lower than) those of other region (without being) contaminated by the nuclear accidents or nuclear reprocessing facilities, which suggests that the ^{129}I inventory is useful to check whether if there are extra sources than global fallout, or others. The $^{129}I/^{127}I$ atomic ratios varied with the water mass flowing in August and October, with higher values (10×10^{-11} to 20×10^{-11}) in the coastal regions of the ECS and lower values ($<8 \times 10^{-11}$) in the offshore. The total inventory of ^{129}I in the water column of the ECS was $(4.2 \pm 0.4) \times 10^{23}$ atoms (~88 g). Contributions from the Changjiang input (<7.5%) and direct atmospheric fallout (<2.7%) to the total ^{129}I in the ECS are much less than the oceanic input from the Yellow Sea via the YSWC and the West Pacific via the KC (the contribution from the Fukushima accident is negligible). These observations suggest that the $^{129}I/^{127}I$ atomic ratios are useful for tracing the of the land-ocean interaction in the marginal seas. The vertical distribution of the $^{129}I/^{127}I$ atomic ratios and salinity are useful for tracing the water mass exchange in the ECS, and the water masses in the ECS present stratification during their confluence; the Changjiang waters could be transported to the North Jiangsu coast both in August and October; and the TWC water could intrude to Northern part of the Changjiang mouth (32°N, 123°E). Besides, the water profiles of iodine isotopes are also helpful to trace the seawater mixing process in ocean marginal systems.

Supplementary data to this article can be found online at https://doi.org/10.1016/j.scitotenv.2018.10.248.

Acknowledgments

This research was supported by the Natural Science Foundation of China (41706089), Ministry of Science and Technology of the People's Republic of China (No. 2015FY110800) and State Key Laboratory of Loess and Quaternary Geology, China. Samples were collected under the support of the Ministry of Science and Technology of PR China (2011CB409801). We appreciate Dr. Qi Liu for his contribution for the measurement of ^{129}I in all samples in Xi'an AMS center.

References

Aldahan, A., Alfimov, V., Possnert, G., 2007a. ^{129}I anthropogenic budget: major sources and sinks. Appl. Geochem. 22 (3), 606–618.
Aldahan, A., Possnert, G., Alfimov, V., Cato, I., Kekli, A., 2007b. Anthropogenic ^{129}I in the Baltic Sea. Nucl. Instrum. Methods Phys. Res., Sect. B 259 (1), 491–495.
Alfimov, V., Aldahan, A., Possnert, G., Winsor, P., 2004a. Anthropogenic iodine-129 in seawater along a transect from the Norwegian coastal current to the North Pole. Mar. Pollut. Bull. 49 (11), 1097–1104.
Alfimov, V., Aldahan, A., Possnert, G., Kekli, A., Meili, M., 2004b. Concentrations of ^{129}I along a transect from the North Atlantic to the Baltic Sea. Nucl. Instrum. Methods Phys. Res., Sect. B 223, 446–450.

Alfimov, V., Aldahan, A., Possnert, G., 2004c. Tracing water masses with ^{129}I in the western Nordic Seas in early spring 2002. Geophys. Res. Lett. 31 (19). https://doi.org/10.1029/2004GL020863.

Alfimov, V., Aldahan, A., Possnert, G., 2013. Water masses and ^{129}I distribution in the Nordic Seas. Nucl. Instrum. Methods Phys. Res., Sect. B 294, 542–546.

Bautista, A.T., Matsuzaki, H., Siringan, F.P., 2016. Historical record of nuclear activities from ^{129}I in corals from the northern hemisphere (Philippines). J. Environ. Radioact. 164, 174–181.

Broecker, W.S., Peng, T.-H., 1982. Tracers in the Sea. Eldigio Press, New York (700 pp.).

Buesseler, K.O., Livingston, H.D., 1997. Time-series profiles of ^{134}Cs, ^{137}Cs and ^{90}Sr in the Black Sea. Sensitivity to Change: Black Sea, Baltic Sea and North Sea. Springer, Dordrecht, pp. 239–251.

Butler, E.C., Smith, J.D., Fisher, N.S., 1981. Influence of phytoplankton on iodine speciation in seawater. Limnol. Oceanogr. 26 (2), 382–386.

Casacuberta, N., Christl, M., Buesseler, K.O., Lau, Y., Vockenhuber, C., Castrillejo, M., ... Masqué, P., 2017. Potential releases of ^{129}I, ^{236}U and Pu isotopes from the Fukushima Dai-ichi nuclear power plants to the ocean during 2013 to 2015. Environ. Sci. Technol. 51 (17), 9826–9835.

Cooper, L.W., Hong, G.H., Beasley, T.M., Grebmeier, J.M., 2001. Iodine-129 concentrations in marginal seas of the North Pacific and Pacific-influenced waters of the Arctic Ocean. Mar. Pollut. Bull. 42 (12), 1347–1356.

Edmonds, H.N., Zhou, Z.Q., Raisbeck, G.M., Yiou, F., Kilius, L., Edmond, J.M., 2001. Distribution and behavior of anthropogenic ^{129}I in water masses ventilating the North Atlantic Ocean. J. Geophys. Res. Oceans 106 (C4), 6881–6894.

Fan, Y., Hou, X., Zhou, W., Liu, G., 2016. ^{129}I record of nuclear activities in marine sediment core from Jiaozhou Bay in China. J. Environ. Radioact. 154, 15–24.

Fehn, U., Snyder, G., Egeberg, P.K., 2000. Dating of pore waters with ^{129}I: relevance for the origin of marine gas hydrates. Science 289, 2332–2335.

Guilderson, T.P., Tumey, S.J., Brown, T.A., Buesseler, K.O., 2014. The 129-iodine content of subtropical Pacific waters: impact of Fukushima and other anthropogenic 129-iodine sources (Biogeosciences). 11, 4839–4852.

Guo, X., Miyazawa, Y., Yamagata, T., 2006. The Kuroshio onshore intrusion along the shelf break of the East China Sea: the origin of the Tsushima Warm Current. J. Phys. Oceanogr. 36 (12), 2205–2231.

He, P., Aldahan, A., Possnert, G., Hou, X.L., 2013a. A summary of global ^{129}I in marine waters. Nucl. Instrum. Methods Phys. Res., Sect. B 294, 537–541.

He, P., Hou, X., Aldahan, A., Possnert, G., Yi, P., 2013b. Iodine isotopes species fingerprinting environmental conditions in surface water along the northeastern Atlantic Ocean. Sci. Rep. 3. https://doi.org/10.1038/srep02685.

He, P., Hou, X., Aldahan, A., Possnert, G., 2014. Radioactive ^{129}I in surface water of the Celtic Sea. J. Radioanal. Nucl. Chem. 299, 249–253.

Hong, G.H., Hamilton, T.F., Baskaran, M., Kenna, T.C., 2012. Applications of anthropogenic radionuclides as tracers to investigate marine environmental processes. Handbook of Environmental Isotope Geochemistry. Springer, Berlin, Heidelberg, pp. 367–394.

Hou, X., Hou, Y., 2012. Analysis of ^{129}I and its application as environmental tracer. J. Anal. Sci. Technol. 3 (2), 135–153.

Hou, X., Dahlgaard, H., Rietz, B., Jacobsen, U., Nielsen, S.P., Aarkrog, A., 1999. Determination of chemical species of iodine in seawater by radiochemical neutron activation analysis combined with ion-exchange preseparation. Anal. Chem. 71 (14), 2745–2750.

Hou, X.L., Dahlgaard, H., Nielsen, S.P., 2000. Iodine-129 time series in Danish, Norwegian and northwest Greenland coast and the Baltic Sea by seaweed. Estuar. Coast. Shelf Sci. 51 (5), 571–584.

Hou, X., Aldahan, A., Nielsen, S.P., Possnert, G., Nies, H., Hedfors, J., 2007. Speciation of ^{129}I and ^{127}I in seawater and implications for sources and transport pathways in the North Sea. Environ. Sci. Technol. 41 (17), 5993–5999.

Hou, X., Hansen, V., Aldahan, A., Possnert, G., Lind, O.C., Lujaniene, G., 2009. A review on speciation of iodine-129 in the environmental and biological samples. Anal. Chim. Acta 632, 181–196.

Hou, X., Zhou, W., Chen, N., Zhang, L., Liu, Q., Luo, M., ... Fu, Y., 2010. Determination of ultralow level ^{129}I/^{127}I in natural samples by separation of microgram carrier free iodine and accelerator mass spectrometry detection. Anal. Chem. 82, 7713–7721.

Hou, X., Povinec, P.P., Zhang, L., Shi, K., Biddulph, D., Chang, C.C., ... Jull, A.T., 2013. Iodine-129 in seawater offshore Fukushima: distribution, inorganic speciation, sources, and budget. Environ. Sci. Technol. 47, 3091–3098.

Huang, D., Du, J., Moore, W.S., Zhang, J., 2013. Particle dynamics of the Changjiang Estuary and adjacent coastal region determined by natural particle-reactive radionuclides (^{7}Be, ^{210}Pb, and ^{234}Th). J. Geophys. Res. Oceans 118 (4), 1736–1748.

Ichikawa, H., Beardsley, R.C., 2002. The current system in the Yellow and East China Seas. J. Oceanogr. 58 (1), 77–92.

Lian, E., Yang, S., Wu, H., Yang, C., Li, C., Liu, J.T., 2016. Kuroshio subsurface water feeds the wintertime Taiwan Warm Current on the inner East China Sea shelf. J. Geophys. Res. Oceans 121 (7), 4790–4803.

Lie, H.J., Cho, C.H., Lee, J.H., Lee, S., Tang, Y., 2000. Seasonal variation of the Cheju warm current in the northern East China Sea. J. Oceanogr. 56 (2), 197–211.

Liu, D., Hou, X., Du, J., Zhang, L., Zhou, W., 2016. ^{129}I and its species in the East China Sea: level, distribution, sources and tracing water masses exchange and movement. Sci. Rep. 6, 36611. https://doi.org/10.1038/srep36611.

Liu, S.M., Qi, X.H., Li, X., Ye, H.R., Wu, Y., Ren, J.L., ... Xu, W.Y., 2016. Nutrient dynamics from the Changjiang (Yangtze River) estuary to the East China Sea. J. Mar. Syst. 154, 15–27.

Liu, J.T., Hsu, R.T., Yang, R.J., Wang, Y.P., Wu, H., Du, X., ... Zhu, J., 2018. A comprehensive sediment dynamics study of a major mud belt system on the inner shelf along an energetic coast. Sci. Rep. 8 (1), 4229. https://doi.org/10.1038/s41598-018-22696-w.

Lu, J., Li, A., Huang, P., Li, Y., 2015. Mineral distributions in surface sediments of the western South Yellow Sea: implications for sediment provenance and transportation. Chin. J. Oceanol. Limnol. 33 (2), 510–524.

Michel, R., Daraoui, A., Gorny, M., Jakob, D., Sachse, R., Tosch, L., ... Stocker, M., 2012. Iodine-129 and iodine-127 in European seawaters and in precipitation from Northern Germany. Sci. Total Environ. 419, 151–169.

Milliman, J.D., Farnsworth, K.L., 2013. River Discharge to the Coastal Ocean: A Global Synthesis. Cambridge University Press, Cambridge (384 pp.).

Oktay, S.D., Santschi, P.H., Moran, J.E., Sharma, P., 2001. ^{129}I and ^{127}I transport in the Mississippi River. Environ. Sci. Technol. 35 (22), 4470–4476.

Povinec, P.P., Livingston, H.D., Shima, S., Aoyama, M., Gastaud, J., Goroncy, I., ... La Rosa, J., 2003. IAEA'97 expedition to the NW Pacific Ocean—results of oceanographic and radionuclide investigations of the water column. Deep-Sea Res. II Top. Stud. Oceanogr. 50 (17–21), 2607–2637.

Povinec, P.P., Lee, S.H., Kwong, L.L.W., Oregioni, B., Jull, A.T., Kieser, W.E., ... Top, Z., 2010. Tritium, radiocarbon, ^{90}Sr and ^{129}I in the Pacific and Indian Oceans. Nucl. Instrum. Methods Phys. Res., Sect. B 268, 1214–1218.

Povinec, P.P., Aoyama, M., Biddulph, D., Breier, R., Buesseler, K., Chang, C.C., ... Kaizer, J., 2011. Tracing of water masses using a multi isotope approach in the southern Indian Ocean. Earth Planet. Sci. Lett. 302, 14–26.

Povinec, P.P., Aoyama, M., Biddulph, D., Breier, R., Buesseler, K., Chang, C.C., ... Kaizer, J., 2013. Cesium, iodine and tritium in NW Pacific waters-a comparison of the Fukushima impact with global fallout. Biogeosciences 10 (8), 5481–5496.

Raisbeck, G.M., Yiou, F., Zhou, Z.Q., Kilius, L.R., 1995. ^{129}I from nuclear fuel reprocessing facilities at Sellafield (UK) and La Hague (France); potential as an oceanographie tracer. J. Mar. Syst. 6 (5–6), 561–570.

Santschi, P.H., Schink, D.R., Corapcioglu, O., Oktay-Marshall, S., Fehn, U., Sharma, P., 1996. Evidence for elevated levels of Iodine-129 in the deep Western Boundary Current in the Middle Atlantic Bight. Deep-Sea Res. I Oceanogr. Res. Pap. 43 (2), 259–265.

Schink, D.R., Santschi, P.H., Corapcioglu, O., Sharma, P., Fehn, U., 1995. ^{129}I in Gulf of Mexico waters. Earth Planet. Sci. Lett. 135 (1–4), 131–138.

Schnabel, C., Olive, V., Atarashi-Andoh, M., Dougans, A., Ellam, R.M., Freeman, S., ... Xu, S., 2007. ^{129}I/^{127}I ratios in Scottish coastal surface sea water: geographical and temporal responses to changing emissions. Appl. Geochem. 22, 619–627.

Schwehr, K.A., Santschi, P.H., Elmore, D., 2005. The dissolved organic iodine species of the isotopic ratio of I-129/I-127: a novel tool for tracing terrestrial organic carbon in the estuarine surface waters of Galveston Bay, Texas. Limnol. Oceanogr. Methods 3, 326–337.

Smith, J.N., Ellis, K.M., Kilius, L.R., 1998. ^{129}I and ^{137}Cs tracer measurements in the Arctic Ocean. Deep-Sea Res. I Oceanogr. Res. Pap. 45 (6), 959–984.

Snyder, G., Aldahan, A., Possnert, G., 2010. Global distribution and long-term fate of anthropogenic ^{129}I in marine and surface water reservoirs. Geochem. Geophys. Geosyst. 11 (doi: 0.1029/2009GC002910).

Suzuki, T., Minakawa, M., Amano, H., Togawa, O., 2010. The vertical profiles of iodine-129 in the Pacific Ocean and the Japan Sea before the routine operation of a new nuclear fuel reprocessing plant. Nucl. Instrum. Methods Phys. Res., Sect. B 268 (7), 1229–1231.

Takata, H., Zheng, J., Tagami, K., Aono, T., Fujita, K., Yamasaki, S.I., ... Uchida, S., 2013. Distribution coefficients (K_d) of stable iodine in estuarine and coastal regions, Japan, and their relationship to salinity and organic carbon in sediments. Environ. Monit. Assess. 185 (5), 3645–3658.

Tan, E., Wang, G., Moore, W.S., Li, Q., Dai, M., 2018. Shelf-scale submarine groundwater discharge in the Northern South China Sea and East China Sea and its geochemical impacts. J. Geophys. Res. Oceans 123 (4), 2997–3013.

Toyama, C., Muramatsu, Y., Igarashi, Y., Aoyama, M., Matsuzaki, H., 2013. Atmospheric fallout of ^{129}I in Japan before the Fukushima accident: regional and global contributions (1963–2005). Environ. Sci. Technol. 47 (15), 8383–8390.

Tumey, S.J., Brown, T.A., Buesseler, K.O., 2014. The 129-iodine content of subtropical Pacific waters: impact of Fukushima and other anthropogenic 129-iodine sources. Biogeosciences 11, 4839–4852.

Wang, J., Du, J., Baskaran, M., Zhang, J., 2016. Mobile mud dynamics in the East China Sea elucidated using ^{210}Pb, ^{137}Cs, ^{7}Be, and ^{234}Th as tracers. J. Geophys. Res. Oceans 121 (1), 224–239.

Wang, J., Baskaran, M., Hou, X., Du, J., Zhang, J., 2017. Historical changes in ^{239}Pu and ^{240}Pu sources in sedimentary records in the East China Sea: implications for provenance and transportation. Earth Planet. Sci. Lett. 466, 32–42.

Wang, X., Baskaran, M., Su, K., Du, J., 2018. The important role of submarine groundwater discharge (SGD) to derive nutrient fluxes into River dominated Ocean Margins–the East China Sea. Mar. Chem. 24, 121–132.

Wu, H., Deng, B., Yuan, R., Hu, J., Gu, J., Shen, F., ... Zhang, J., 2013. Detiding measurement on transport of the Changjiang-derived buoyant coastal current. J. Phys. Oceanogr. 43 (11), 2388–2399.

Wu, H., Shen, J., Zhu, J., Zhang, J., Li, L., 2014. Characteristics of the Changjiang plume and its extension along the Jiangsu Coast. Cont. Shelf Res. 76, 108–123.

Wu, J., Zheng, J., Dai, M., Huh, C.A., Chen, W., Tagami, K., Uchida, S., 2014. Isotopic composition and distribution of plutonium in northern South China Sea sediments revealed continuous release and transport of Pu from the Marshall Islands. Environ. Sci. Technol. 48 (6), 3136–3144.

Xing, S., Hou, X., Aldahan, A., Possnert, G., Shi, K., Yi, P., Zhou, W., 2017. Water circulation and marine environment in the Antarctic traced by speciation of ^{129}I and ^{127}I. Sci. Rep. 7 (1), 7726. https://doi.org/10.1038/s41598-017-07765-w.

Yang, S.L., Xu, K.H., Milliman, J.D., Yang, H.F., Wu, C.S., 2015. Decline of Yangtze River water and sediment discharge: impact from natural and anthropogenic changes. Sci. Rep. 5, 12581. https://doi.org/10.1038/srep12581.

Yi, P., Aldahan, A., Hansen, V., Possnert, G., Hou, X.L., 2010. Iodine isotopes (^{129}I and ^{127}I) in the Baltic Proper, Kattegat, and Skagerrak basins. Environ. Sci. Technol. 45 (3), 903–909.

Zhang, L.Y., Hou, X.L., 2013. Speciation analysis of ^{129}I and its applications in environmental research. Radiochim. Acta 101 (8), 525–540.

Zhang, W., Ma, H., Ye, L., Dong, C., Yu, L., Feng, H., 2012. Magnetic and geochemical evidence of Yellow and Yangtze River influence on tidal flat deposits in northern Jiangsu Plain, China. Mar. Geol. 319, 47–56.

Zhang, J., Guo, X., Zhao, L., Miyazawa, Y., Sun, Q., 2017. Water exchange across isobaths over the continental shelf of the East China Sea. J. Phys. Oceanogr. 47 (5), 1043–1060.

Zhang, L., Hou, X., Li, H.C., Xu, X., 2018. A 60-year record of ^{129}I in Taal Lake sediments (Philippines): influence of human nuclear activities at low latitude regions. Chemosphere 193, 1149–1156.

Zhao, L., Liu, D., Wang, J., Du, J., Hou, X., Jiang, Y., 2018. Spatial and vertical distribution of radiocesium in seawater of the East China Sea. Mar. Pollut. Bull. 128, 361–368.